http://doi.org/10.1093/plcell/koab270 THE PLANT CELL 2022: 34: 616–632

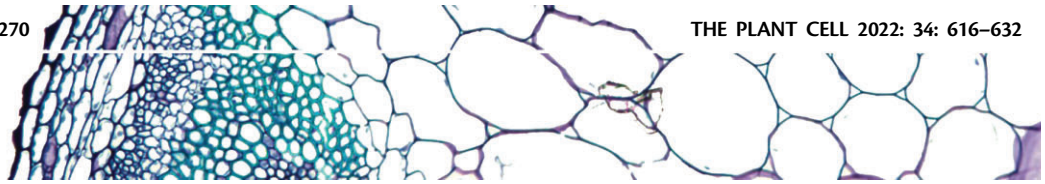

Research Article

The evolutionarily conserved kinase SnRK1 orchestrates resource mobilization during Arabidopsis seedling establishment

Markus Henninger [1], **Lorenzo Pedrotti** [1], **Markus Krischke** [1], **Jan Draken** [1], **Theresa Wildenhain** [1], **Agnes Fekete** [1], **Filip Rolland** [2,3], **Martin J. Müller** [1], **Christian Fröschel** [1], **Christoph Weiste** [1] and **Wolfgang Dröge-Laser** [1,*,†]

1 Department of Pharmaceutical Biology, Julius-von-Sachs-Institute, Julius-Maximilians-Universität Würzburg, 97082 Würzburg, Germany
2 Laboratory of Molecular Plant Biology, Department of Biology, KU Leuven, B-3001 Leuven, Belgium
3 KU Leuven Plant Institute (LPI), KU Leuven, B-3001 Leuven, Belgium

*Author for correspondence: wolfgang.droege-laser@uni-wuerzburg.de
†Senior author.

M.H. and W.D.L established the research plan and interpreted the results. M.H. performed most of the experiments. L.P. conducted initial experiment providing the basis for the project. C.W. assisted the work on ChIP and protoplasts, F.R. and J.D. provided material and performed kinase assay, T.W. and C.F. performed additional mutant analyses and qRT-PCR experiments, M.M, M.K. and A.F guided and assisted in metabolite measurements. M.H. is responsible for bioinformatical calculations and analyses of RNAseq data. W.D.L., C.W., and M.H. prepared the figures and wrote the manuscript. All authors discussed the results and commented on the manuscript.

The author responsible for distribution of materials integral to the findings presented in this article in accordance with the policy described in the Instructions for Authors (https://academic.oup.com/plcell) is: Wolfgang Dröge-Laser (wolfgang.droege-laser@uni-wuerzburg.de)

Abstract

The onset of plant life is characterized by a major phase transition. During early heterotrophic seedling establishment, seed storage reserves fuel metabolic demands, allowing the plant to switch to autotrophic metabolism. Although metabolic pathways leading to storage compound mobilization are well-described, the regulatory circuits remain largely unresolved. Using an inducible knockdown approach of the evolutionarily conserved energy master regulator Snf1-RELATED-PROTEIN-KINASE1 (SnRK1), phenotypic studies reveal its crucial function in *Arabidopsis thaliana* seedling establishment. Importantly, glucose feeding largely restores growth defects of the kinase mutant, supporting its major impact in resource mobilization. Detailed metabolite studies reveal sucrose as a primary resource early in seedling establishment, in a SnRK1-independent manner. Later, SnRK1 orchestrates catabolism of triacylglycerols and amino acids. Concurrent transcriptomic studies highlight SnRK1 functions in controlling metabolic hubs fuelling gluconeogenesis, as exemplified by cytosolic PYRUVATE *ORTHO*PHOSPHATE DIKINASE (cyPPDK). Here, SnRK1 establishes its function via phosphorylation of the transcription factor BASIC LEUCINE ZIPPER63 (bZIP63), which directly targets and activates the *cyPPDK* promoter. Taken together, our results disclose developmental and catabolic functions of SnRK1 in seed storage mobilization and describe a prototypic gene regulatory mechanism. As seedling establishment is important for plant vigor and crop yield, our findings are of agronomical importance.

Received June 28, 2021. Accepted October 28, 2021. Advance access publication November 10, 2021

Introduction

Seed germination and subsequent seedling establishment are entirely heterotrophic and seed storage reserves are mobilized to sustain metabolic demands until the photosynthetic apparatus is established to implement an autotrophic lifestyle (Graham, 2008; Quettier and Eastmond, 2009; Tan-Wilson and Wilson, 2012). While enzymatic activities in resource mobilization are well-described, knowledge of the regulatory co-ordination of resource mobilization lags behind. Hence, reserve mobilization during seedling establishment is a valuable model system to study metabolic regulation and more importantly, is crucial for crop yield in agriculture.

Carbohydrates, proteins, and lipids are well-known seed storage compounds. Whereas cereals preferentially store starch, legumes use proteins and Brassicaceae, such as *Arabidopsis thaliana*, favor lipids (Graham, 2008). Lipids are stored in oil bodies as triacylglycerols (TAGs) and are broken down to fatty acids (FAs) and glycerol (Graham, 2008; Li-Beisson et al., 2013). Both products are used as substrates for gluconeogenesis and hence support heterotrophic energy metabolism (Baker et al., 2006). SUGAR-DEPENDENT1 (SDP1) and SDP1-LIKE1 are the major lipases involved in FA release from TAG stores during germination (Eastmond, 2006; Quettier and Eastmond, 2009). After import into peroxisomes, FAs are degraded via β-oxidation to generate acetyl-coenzyme A (Ac-CoA; Baker et al., 2006; Pan et al., 2020). Here, PEROXISOMAL MALATE DEHYDROGENASE1/2 (PMDH1/2) is crucial to re-oxidize NADH and thereby facilitate continuous operation of β-oxidation (Pracharoenwattana et al., 2007, 2010). In contrast to mammals, the glyoxylate cycle in plant peroxisomes then makes use of this Ac-CoA to generate dicarboxylic acids, which are shuttled into gluconeogenesis. In a plant-specific pathway, phosphoenolpyruvate (PEP) is produced from oxaloacetate by PYRUVATE CARBOXYKINASE1 (PCK1), an essential enzyme in seedling establishment (Rylott et al., 2003; Penfield et al., 2004; Eastmond et al., 2015).

Besides lipids, seed storage proteins (SSPs) perform as a second important resource in Arabidopsis (Alonso et al., 2009; Tan-Wilson and Wilson, 2012). After proteolytic breakdown of SSPs, carbon skeletons derived from amino acids (AAs) are similarly channeled into gluconeogenesis via PEP. Recently, PYRUVATE *ORTHO*PHOSPHATE DIKINASE (PPDK) has been demonstrated as a key enzyme in this second pathway in Arabidopsis (Eastmond et al., 2015). PPDK catalyzes the production of PEP from pyruvate, resulting from the breakdown of several AAs. In Arabidopsis, a chloroplastic (cp) and a cytosolic (cy) PPDK isoform are derived from a single gene, as production of the latter is controlled by transcription from an alternative promoter in the first intron (Parsley and Hibberd, 2006). Expression studies and mutant analyses disclosed that both PCK1 and cyPPDK are important metabolic hubs, required for seedling establishment, supplying gluconeogenesis using complementary TAG and AA resources (Eastmond et al., 2015).

While starch is an important storage resource in cereals, its content in Arabidopsis seeds is neglectable. Sucrose is available, but is not well studied as a resource for seedling establishment (Silva et al., 2017).

Regulation of storage resource mobilization requires metabolic sensing of crucial compounds and sophisticated signaling networks to integrate metabolic demands, developmental programs, and environmental cues. In eukaryotes, energy and resource homeostasis is controlled by a pair of evolutionarily conserved master kinases. In a simplistic view, TARGET OF RAPAMYCIN (TOR) activates anabolic metabolism related to growth and development, whereas yeast Sucrose non-fermenting 1 (Snf1), mammalian AMP-activated protein kinase (AMPK) and plant Snf1-RELATED PROTEIN KINASE1 (SnRK1) stimulate catabolic and energy-preserving processes (Baena-González et al., 2007; Hardie, 2015; Crepin and Rolland, 2019). During Arabidopsis seedling establishment, TOR positively controls growth by activating the root apical meristem (Xiong et al., 2013). Due to its catabolic function, SnRK1 is anticipated to be involved in resource mobilization in this developmental transition.

Structurally, the SnRK1 complex consists of a catalytic α-subunit and regulatory β- and γ-subunits (Baena-González and Sheen, 2008; Broeckx et al., 2016; Emanuelle et al., 2016; Crepin and Rolland, 2019). Analysis of SnRK1 function is complicated by a combinatorial complexity, as all subunits are encoded by small gene families and multiple cellular localizations are described (Blanco et al., 2019). In Arabidopsis three genes encode catalytic α-subunits, *SnRK1α1* (*AKIN10*), *SnRK1α2* (*AKIN11*), and *SnRK1α3* (*AKIN12*; Baena-González et al., 2007). *SnRK1α3* is hardly expressed, but *SnRK1α1* and *SnRK1α2* are essential and partially redundant. Whereas mammalian AMPK directly responds to cellular changes in AMP/ATP ratios, affecting T-loop phosphorylation of the catalytic subunit, this mechanism apparently does not function in plants (Emanuelle et al., 2015).

Accumulating evidence supports the view that glucose (Glc) sensing may be the ancestral role of the Snf1/SnRK1/AMPK system (Lin and Hardie, 2017) and in plants sugar-phosphates, such as glucose-6-P and trehalose-6-P, were proposed as allosteric inhibitors of SnRK1 activity (Nunes et al., 2013; Zhai et al., 2018). Together with a strong T-loop autophosphorylation activity, these data suggest a plant-specific SnRK1 regulatory mechanism, which is based on an active (derepressed) state as default (Crepin and Rolland, 2019). Moreover, metabolic stress-induced nuclear translocation of the catalytic α-subunit is proposed to be required for target gene induction (Ramon et al., 2019). Upon low-energy stress, the α-subunit is recruited to the chromatin of targeted genes via transcription factor (TF) adapters, such as BASIC LEUCINE ZIPPER63 (bZIP63; Pedrotti et al., 2018).

Phospho-proteomic and transcriptomic approaches have established the massive regulatory impact of SnRK1 by phosphorylating metabolic enzymes or signaling molecules, such as TFs (Nukarinen et al., 2016). SnRK1 is implicated in a

plethora of developmental processes, from seed maturation to flowering and senescence, as well as the induction of alternative metabolic pathways to survive low energy-related stresses. However, only limited data is available on SnRK1 function in seedling development, such as in sucrose-induced hypocotyl elongation (Simon et al., 2018) or impact on root growth (Baena-González et al., 2007).

Here, we disclose a crucial function of SnRK1 in Arabidopsis seedling establishment and particularly resource mobilization using inducible knockdown of the SnRK1 catalytic α-subunits. Feeding the mutant with glucose largely restores growth and developmental defects, suggesting a metabolic block in storage resource mobilization, related to the absence of active SnRK1. This notion is supported by quantifying lipid, carbohydrate, and AA contents throughout seedling establishment. A pivotal role of SnRK1 in AA and TAG metabolism is further underlined by transcriptome studies, defining a SnRK1-dependent transcriptional regulation of major metabolic hubs, such as PCK1, cyPPDK, and PMDH2. With respect to regulation of cy*PPDK* in fuelling gluconeogenesis, we identified the TF bZIP63 as a SnRK1 kinase downstream target, directly binding and regulating the cy*PPDK* promoter. Taking these findings together, this study discloses a function of SnRK1 as a central regulator in seed storage compound breakdown and provides a mechanistic mode of action.

Results

SnRK1 is essential for Arabidopsis seedling establishment

To assess SnRK1 function during seedling establishment, we made use of an inducible loss-of-function approach for the genes encoding the catalytic SnRK1α1 and SnRK1α2 subunits. As a double mutant is lethal (Baena-González et al., 2007), we expressed an estradiol (Est)-inducible artificial microRNA (amiR), targeting *SnRK1α2* in a *snrk1α1* mutant background (*snrk1α1/α2*; Pedrotti et al., 2018). Seeds were germinated and cultured according to the scheme depicted in Figure 1A. To mimic natural situations, we started a heterotrophic culture in darkness to induce storage compound breakdown. The etiolated seedlings were shifted to a 12-h/12-h day/night regime 3 days after germination (DAG) and the growth phenotype was documented until 7 DAG (Figure 1A).

To confirm the efficiency of the knockdown approach, protein levels of SnRK1α1 and SnRK1α2 were assayed during the time course by immunoblotting (Figure 1B). While protein levels of both kinase subunits were below the detection limit in the double mutant, the highest SnRK1α1 and SnRK1α2 levels were observed in the Columbia-0 (Col-0) wild-type (WT) 2–3 DAG in darkness. These expression data propose a potential time frame of SnRK1 function, presumably reflecting limiting resources in the heterotrophic seedling. Quantification of the phenotypes by measuring fresh weight (Figure 1C) revealed no difference between WT and the single mutants. In contrast, the *snrk1α1/α2* double mutant was significantly impaired in growth. In addition, we assessed the impact of SnRK1 on the growth of etiolated seedlings in a persistent heterotrophic system. Again, fresh weight of seedlings grown under constant darkness was severely reduced in *snrk1α1/α2* (Supplemental Figure S1A).

Although a significant increase in chlorophyll content was observed in all plants tested after a shift to light, in the double mutant this increase was transient and levels declined again 5 DAG (Figure 1D). To further characterize changes in the development of the photosynthetic apparatus during the shift from heterotrophy to autotrophy, we measured chlorophyll fluorescence (F_v/F_m). In WT, photosynthesis was fully active already 4–6 h after the shift to light (Supplemental Figure S1B) and remained constant within the 7-day time frame of the experiment (Figure 1E). In contrast, the chlorophyll fluorescence of the double mutant only transiently increased upon light exposure and then continued to decline until 7 DAG. Accordingly, transcript abundance of *GOLDEN-LIKE2* (*GLK2*), a central transcriptional regulator and marker of chloroplast development (Waters et al., 2009) was significantly reduced in *snrk1α1/α2* in comparison to WT (Figure 1F). Therefore, a substantial reduction in the expression of SnRK1 catalytic subunits strongly impaired seedling establishment in darkness as well as transition to photo-autotrophic growth.

The *snrk1α1/α2* loss-of-function phenotype in seedling establishment can be rescued by supplementing metabolizable sugars

As SnRK1 is proposed to be a master regulator of catabolic processes, the dramatic growth phenotype might be due to a pleiotropic impact on numerous metabolic pathways (Baena-González et al., 2007). As sugar feeding has successfully been used to recover mutants in storage resource mobilization (Eastmond, 2006), we reasoned that the phenotype might be rescued by supplementing specific metabolites, to determine those compounds which are limiting mutant growth. As depicted in Figure 2A, Glc (3%) feeding stimulates growth and partially or fully rescues fresh weight or chlorophyll content, respectively (Figure 2, B and C). Feeding low Glc concentrations (0.5%) or other sugars such as sucrose (Suc) and galactose (Gal) were found to rescue chlorophyll content in the mutant (Figure 2D), whereas the non-metabolizable sugar 3-*ortho*-methyl-glucose (3-OMG) or the osmotic control mannitol did not (Cortés et al., 2003). This is in line with the well-established knowledge that Glc functions as a central carbohydrate in energy metabolism but additionally performs as a signal in controlling gene expression and development (Skylar et al., 2011; Yu et al., 2013). This is an important finding, as these data support the view that the *snrk1α1/α2* mutant phenotype is primarily due to mis-regulation of specific catabolic pathways in resource mobilization.

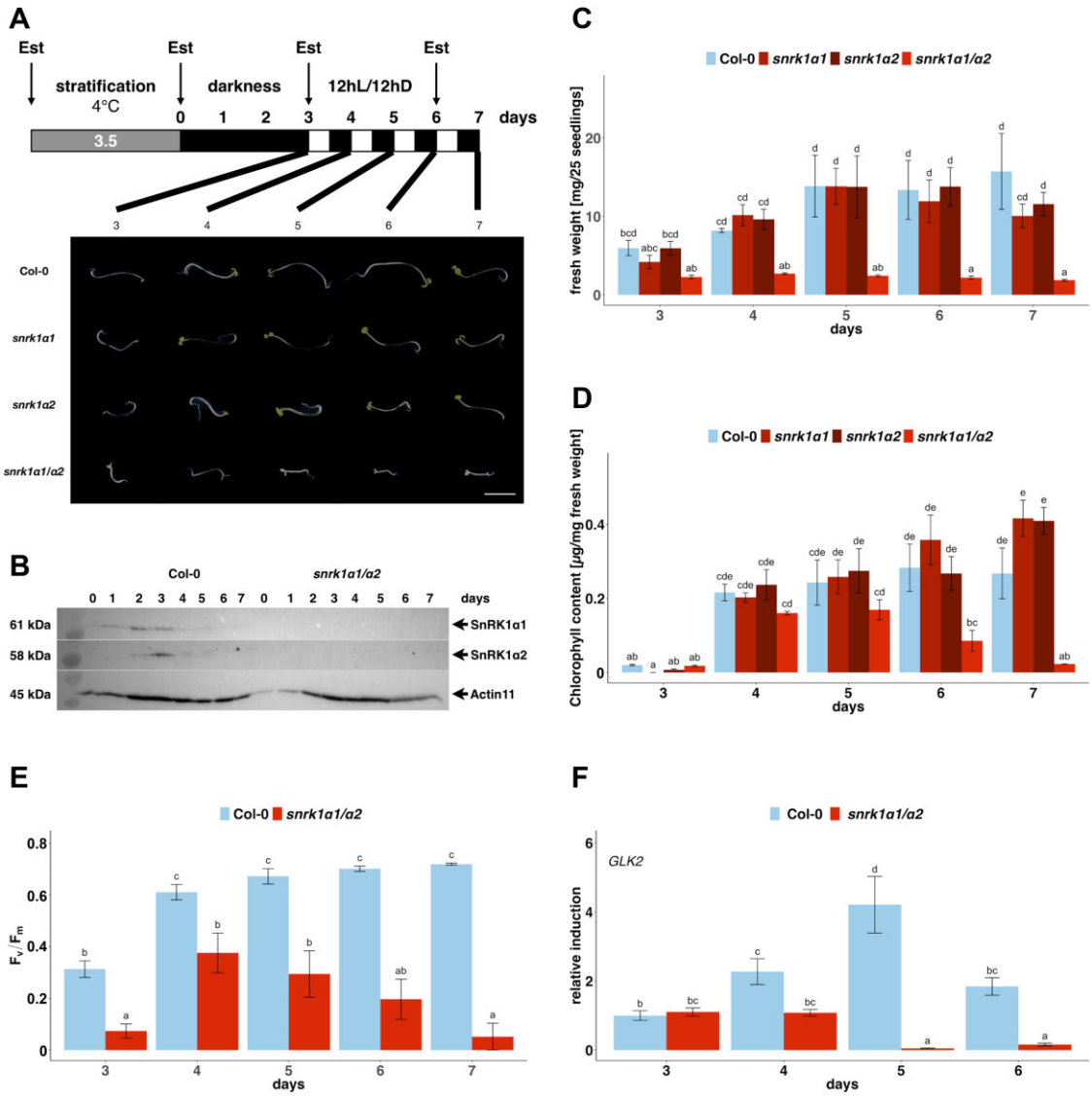

Figure 1 SnRK1 is required for seedling establishment. A, Schematic representation of the experimental set up. WT (Col-0), *snrk1α1*, *snrk1α2*, and Est inducible *snrk1α1/α2* mutant seedlings were aseptically cultivated in liquid-MS medium. After stratification for 3.5 days, seeds were cultivated at 21°C in darkness for 3 days and subsequently shifted to a 12-h/12-h day/night regime until 7 DAG. Est (10 µM) was added every 3 days to WT and mutant lines. At the indicated time points, samples were harvested at the end of the night and representative photos were taken. Bar: 20 mm. B, Immunoblot detection of SnRK1α1 and SnRK1α2 in WT and the *snrk1α1/α2* mutant at the end of the night. Equal loading was controlled using immunostaining of ACTIN11. C, D, Quantification of fresh weight (C) or chlorophyll content (D) of seedlings cultured according to the experimental set up in (A). WT (blue), *snrk1α1* and *snrk1α2* single mutants (brown) or double mutant (red). E, Photosynthetic efficiency measured by pulse-amplitude modulated fluorometry for WT and *snrk1α1/α2* seedlings, 4 h after onset of light (n = 12). F, Transcript abundance of the *GLK2* marker for chloroplast development (Waters et al., 2009), as measured by qRT-PCR. A–F, Given are mean values of three biological replicates derived from pools of 25 seedlings ± standard error of the mean (SEM). Significant differences between treatments are designated by different letters (one-way ANOVA with Bonferroni–Holm post hoc test; $P < 0.05$). The experiments were repeated three times with similar results.

Mobilization of storage compounds such as TAGs or AAs use canonical pathways to fuel energy metabolism with Glc through gluconeogenesis

To obtain further insights into the metabolic block(s), we supplemented the *snrk1α1/α2* mutant with metabolites related to specific pathways such as short-chain FAs, dicarboxylic acids, or proteogenic AAs, none of which rescued the chlorophyll content of the mutant (Supplemental Figure S2, A–C). It needs to be noted, that although uptake of FAs and functional supplementation by AAs has been demonstrated in plants (Tjellström et al., 2015; Pedrotti et al., 2018), the efficiency of these feeding experiments has not been assessed. Nevertheless, these findings may suggest that several SnRK1-regulated catabolic pathways are involved in Glc-dependent energy metabolism.

To substantiate the phenotypic data, we performed RNA-sequencing (RNA-seq) of WT and *snrk1α1/α2* seedlings after

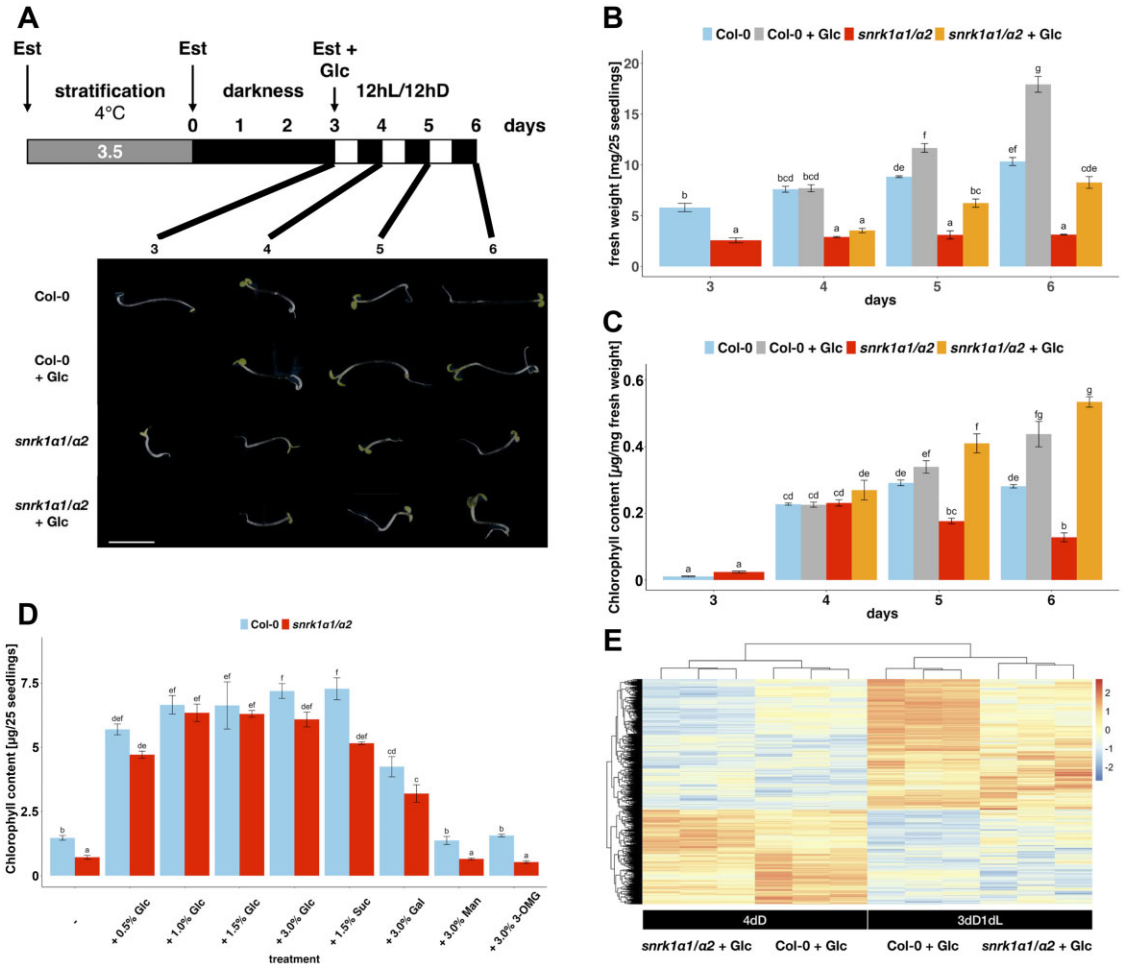

Figure 2 Feeding of metabolizable sugars partially rescues the *snrk1α1/α2* mutant phenotype. A, Schematic view of the experimental set up. Glc (final concentration 3%) was added to the medium after culture of seedlings for 3 dD. Given are representative photos taken at the end of the night for the time points indicated. Bar: 20 mm. B, C, Determination of fresh weight (B) or chlorophyll content (C) of WT (blue) and *snrk1α1/α2* (red) seedlings without sugar or after Glc treatment, respectively (gray or orange) at the time points indicated. D, Quantification of chlorophyll content 7 DAG. Samples were treated with the indicated sugars on day 3. Given are mean values of three biological replicates derived from a pool of 25 seedlings each ±SEM. Significant differences between treatments are designated by different letters (one-way ANOVA with Bonferroni–Holm post hoc test; $P < 0.05$). E, Hierarchical clustering of genes displaying differential expression among samples as determined by RNAseq ($P < 0.05$, log2 FC $\leqslant$ 2). Compared are three replicates of Col-0 and *snrk1α1/α2* seedlings after Glc treatment 3 DAG relative to the mean of all samples. As depicted in the scheme, transcriptomes were studied after 4 days in darkness (4 dD) or 3 days in darkness and 1 day in 12-h/12-h day/night regime (3 dD 1dL), respectively. Given are color-coded log2 FC values of up- (red) or downregulated (blue) genes.

Glc feeding (Figure 2A). Feeding occured 3 DAG and samples were harvested either after 24-h in darkness (4 dD) or light (3 dD 1dL). Although differential gene expression patterns could be observed between WT and *snrk1α1/α2* seedlings (Supplemental Data Set S1), hierarchical clustering (Figure 2E) surprisingly displayed rather limited SnRK1-dependent differences when compared to data from plants without Glc treatment (Figure 3, A–D). Taken together, phenotypic and molecular data support the view that during early seedling development, SnRK1 primarily acts on the level of resource mobilization and therefore, we focused on this aspect.

The *snrk1α1/α2* mutant shows a massive transcriptional deregulation during seedling establishment

To obtain a deeper insight into SnRK1-dependent processes during seedling establishment and storage compound mobilization, combined transcriptome and metabolite studies were performed (Supplemental Data Set S1). In time-course experiments, transcripts isolated from WT and *snrk1α1/α2* mutant seedlings were compared, both during continued darkness (3 dD–5 dD; Figure 3, A and B) or after shifting them from darkness (3 dD) to a 12-h/12-h day/night regime for 1 or 2 additional days (3 dD 1dL, 3 dD 2dL; Figure 3, C

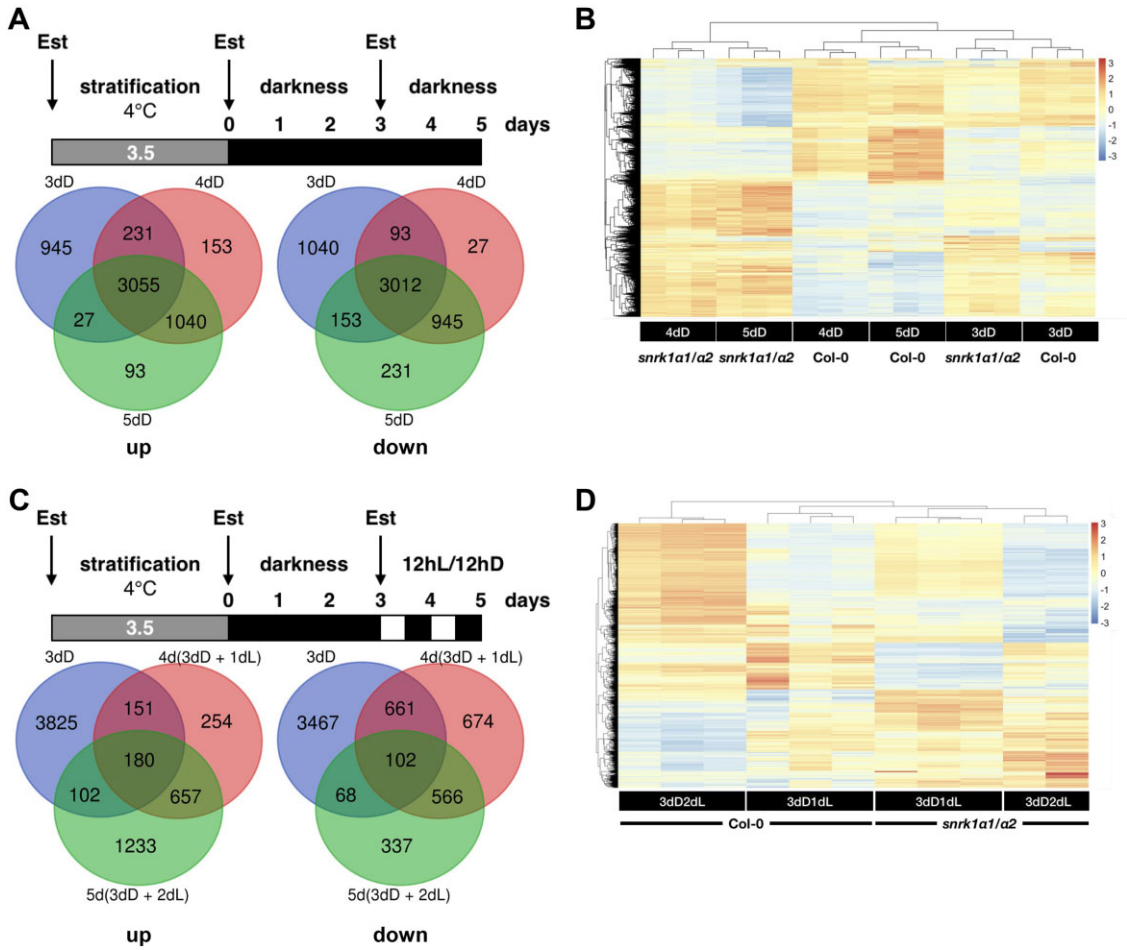

Figure 3 Transcriptome analyses comparing WT and the *snrk1α1/α2* mutant during seedling establishment. A–D, RNAseq time-course experiments comparing WT (Col-0) and *snrk1α1/α2* seedlings during darkness (3 dD, 4 dD, 5 dD) (A and B) or after shift to 12-h/12-h day/night regime on day 3 (3 dD 1dL, 3 dD 2dL) (C and D). Up- and downregulated DEGs ($P < 0.01$, log2 FC $\leqslant 2$) are presented by Venn diagrams (A and C) or color-coded hierarchical clustering of three biological replicates displaying differential expression among samples (B and D).

and D). As depicted in the Venn diagrams (Figure 3A), approximately 3,000 up- as well as downregulated differential expressed genes (DEGs; $\log_2$ fold change (FC); $P \leqslant 0.01$) were shared at all analyzed time points in continued darkness. The massive transcriptional regulation observed in the mutant is in line with previously published data obtained from leaves (Pedrotti et al., 2018) or overexpression in protoplast (Baena-González et al., 2007). Accordingly, these findings underline the crucial role of SnRK1 in controlling gene expression in seedling establishment. A detailed cluster analysis (Figure 3B) revealed an increasing impact of SnRK1 on gene expression particularly at later time points (4 dD, 5 dD).

As demonstrated in Figure 3C, only small sets of 180 and 102 up- and downregulated SnRK1-dependent genes are common in etiolated seedlings at 3 DAG and after shifting to day/night rhythm. This is conceivable, since transition to the autotrophic lifestyle leads to a massive transcriptional reprogramming (Xiong et al., 2013; Silva et al., 2016). Similarly, 254 and 1,233 SnRK1-dependent genes were upregulated specifically at the 3 dD 1dL or 3 dD 2dL time points, respectively.

These results support the idea that SnRK1 impacts gene expression both in etiolated seedlings and during photomorphogenesis. Importantly, the DEG collections under light and dark conditions differ considerably. A detailed overview can be found in Supplemental Data Set S1. DEGs related to storage compound catabolism were explored further.

SnRK1 is required for mobilization of TAG reserves during late seedling establishment

To study SnRK1-dependent resource mobilization, we compared transcriptome and metabolic data (Supplemental Data Set S2) in detailed time-course experiments. Although classified as an oil-plant, Arabidopsis is not using lipids as a primary resource, as the overall TAG content did not change substantially during the first 3 dD. Interestingly, no differences were observed between WT and the *snrk1α1/α2* mutant (Figure 4A). After 3 days, TAG levels decreased rapidly in WT, independent of dark or light cultivation. These findings indicated that Arabidopsis is financing early growth of etiolated seedling by other resources, which are later replaced by TAGs. Interestingly, TAG breakdown requires

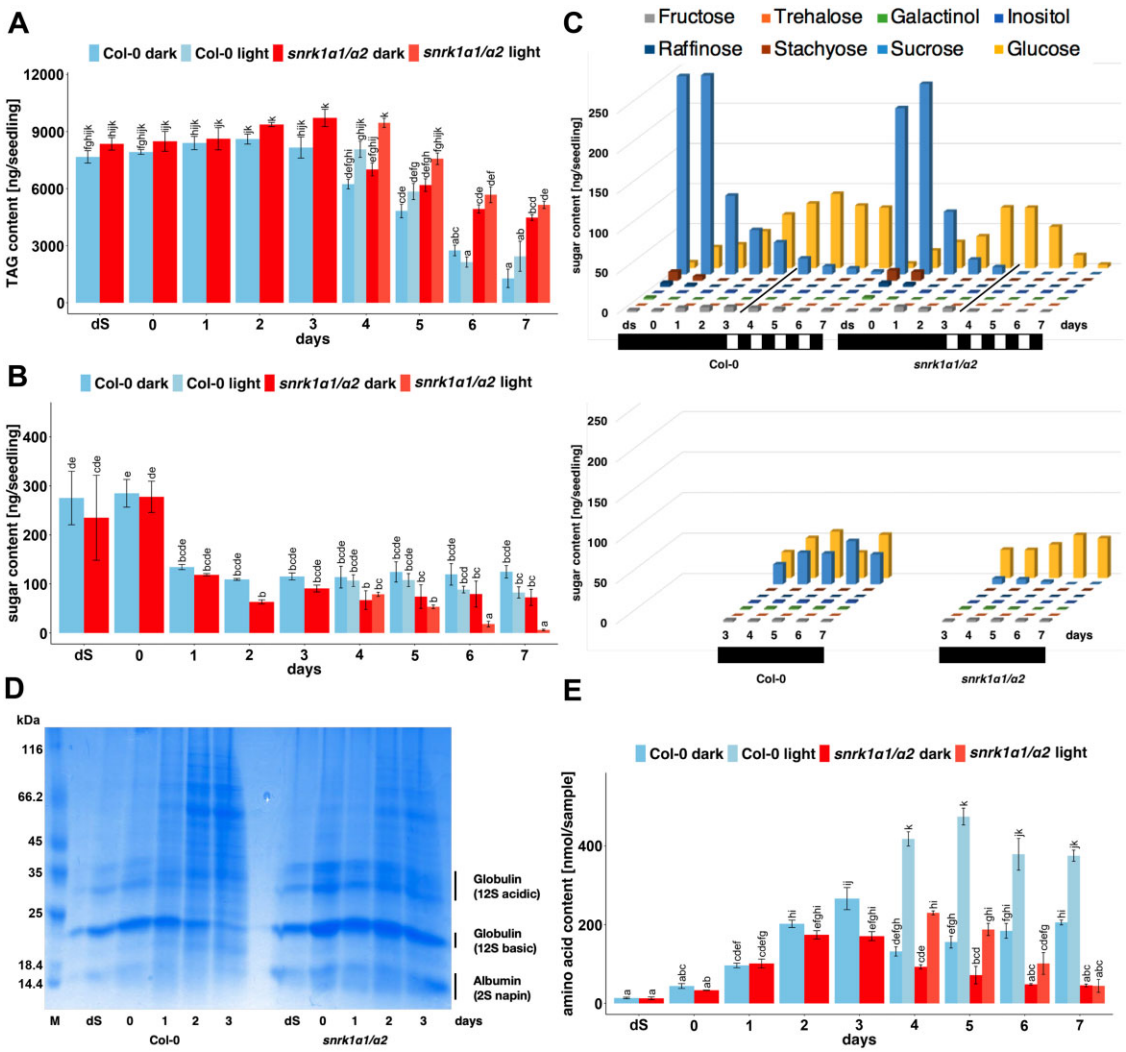

Figure 4 SnRK1-dependent mobilization of seed storage compounds during seedling establishment. A and B, Analysis of total TAG (A) and the total content of determined sugars (B) of dry seeds (ds) and seedlings up to 7 DAG. Compared are WT (Col-0) in constant darkness (dark blue) or 3 dD followed by 12-h/12-h day/night regime (light blue) or the respective *snrk1α1/α2* mutant in red and orange. C, Detailed display of sugars summarized in (B) as depicted by the color code. Cultivation in light (upper panel) or constant darkness (lower panel) as well as timelines are provided. D, Major SSPs of WT and *snrk1α1/α2* dry seeds (ds) or seedlings displayed by SDS–PAGE and Coomassie staining during culture in constant darkness. Time points are indicated. E, Total AA content of ds and seedlings up to 7 DAG. Compared are WT (Col-0) in darkness (dark blue) or 3 dD followed by 12-h/12-h day/night regime (light blue) or the respective *snrk1α1/α2* mutant (red and orange). A–C, and E, Given are mean values of three biological replicates harvested at the end of night derived from 25 seedlings ±SEM. Significant differences between treatments are designated by different letters (one-way ANOVA with Bonferroni–Holm post hoc test; $P < 0.05$).

SnRK1 as the *snrk1α1/α2* mutant retained substantially higher TAG levels even 7 DAG.

Besides total TAG measurements, a detailed analysis of specific TAGs revealed an enrichment of highly unsaturated FA with 52–54 carbon-atoms (Supplemental Figure S3A). The metabolic data were correlated with transcriptome data provided by a MapMan representation (Schwacke et al., 2019; Supplemental Figure S3B). Gene expression particularly related to TAG and FA biosynthesis was downregulated in the *snrk1α1/α2* mutant, which may be indirectly regulated by the high amounts of remaining TAGs. As summarized in the metabolic overview in Figure 5, only limited DEGs related to TAG breakdown were transcriptionally downregulated in a SnRK1-dependent manner, more specifically *ACYL-COA OXIDASE* (*ACX4*) and *PMDH2* both in darkness and light and *PCK1* only in darkness. Interestingly, most genes related to TAG mobilization, β-oxidation, glyoxylate cycle, or gluconeogenesis showed minor or no SnRK1-dependent transcription (Figure 5; Supplemental Data Set S1), supporting a preferentially nontranscriptional control of TAG catabolism.

Sucrose fuels early seedling establishment independently of SnRK1

Next, we assayed carbohydrates, which may serve as an alternative storage resource. Consistent with published data, Arabidopsis seeds do not store starch but instead a substantial amount of Suc, which has been described as a primary resource (Footitt et al., 2002). We therefore measured

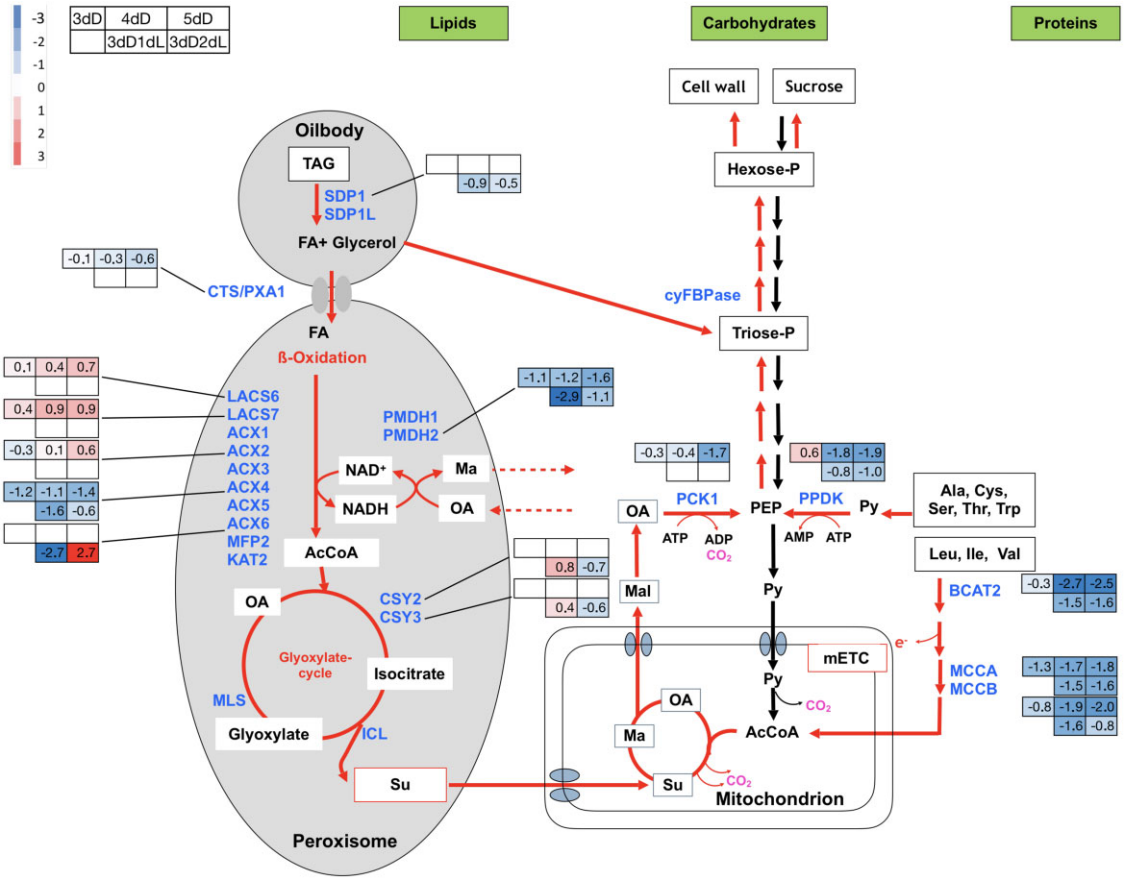

Figure 5 Schematic overview of SnRK1-dependent differentially expressed genes related to storage compound mobilization. TAG degradation, β-oxidation, glyoxylate cycle, TCA cycle, glycolysis, gluconeogenesis, and AA catabolism are depicted. The log2 FC of genes selected from the RNAseq dataset (Supplementary Table S1) are color-coded: down- (blue), up- (red) nonregulated ($P < 0.05$; white) in *snrk1α1/α2* mutant in comparison to WT. Time points after 3D, 4D, 5D and after shift to 12-h/12-h day/night regime for 4–5 days (3 dD 1dL, 3 dD 2dL) were analyzed. AcCoA, acetyl-coenzyme A; OA, oxaloacetate; Su, succinate; Mal, malate; Py, pyruvate; P, phosphate; ATP/ADP/AMP, adenosintri-/di-/monophosphate; Ala, alanine; Cys, cysteine; Ser, serine; Thr, threonine; Trp, tryptophan; Leu, leucine; Ile, isoleucine; Val, valine; gene names are mentioned in the text.

changes in total and specific soluble sugar levels (Figure 4, B and C). During the first 3 dD, Suc levels declined in WT and the *snrk1α1/α2* mutant in a comparable manner, suggesting a SnRK1-independent control of Suc usage during etiolated seedling. Although Glc and Fructose (Fru) should be derived from the cleavage of Suc, only Glc was found in substantial amounts, increasing steadily until 3 DAG and staying constant in WT and *snrk1α1/α2* mutant until 5 DAG. Consistent with the transcriptome data, no impact of SnRK1 on this carbohydrate metabolism was observed. In contrast to these early time points, Glc levels in the *snrk1α1/α2* mutant are completely exhausted in the *snrk1α1/α2* mutant at 7 DAG, which correlates with impairment in growth. This sudden drop in Glc levels in the *snrk1α1/α2* mutant may be due to the lack of Glc derived from other resources such as TAGs or AAs. Interestingly, the WT and *snrk1α1/α2* mutant maintained low levels of Glc in the darkness, as they are not investing in photomorphogenesis. However, Suc was found to be limited in the *snrk1α1/α2* mutant in comparison to WT. Taken together, probably via its conversion into Glc, Suc supports early etiolated seedling growth largely independently of SnRK1. Accordingly, almost no changes in carbohydrate-related gene expression were observed (Supplemental Data Set S1).

SnRK1 severely impacts AA metabolism during seedling establishment

During early seedling development, AAs are derived from degradation of storage proteins. As depicted in the protein gel in Figure 4D, degradation of storage proteins was initiated in WT plants 1–3 DAG but was significantly delayed in the *snrk1α1/α2* mutant, particularly visible for globulins. This finding was also reflected in total AA levels in the *snrk1α1/α2* mutant at 3DAG (Figure 4E). In contrast to a limited decrease of total AA levels in constant darkness, AA concentration significantly increased in light, presumably due to light-driven biosynthesis. However, during the analyzed time course, total AA levels significantly declined in the *snrk1α1/α2* mutant, both in constant darkness and day/night regime. A detailed view of individual AA pools is provided in Supplemental Figure S4, A and B. Due to storage protein degradation, most of the AAs were measured in substantial

amounts 2–3 DAG, both in WT and *snrk1α1/α2* mutant. Strikingly, Gln and Asn levels, which are important transport forms of nitrogen and carbon (Lam et al., 2003) significantly increased after the shift to light and strongly decreased in *snrk1α1/α2* mutant up to day 7 (Supplemental Figure S4). This is also the case in continued darkness, but at a lower level. The high levels of particular AAs cannot be derived from catabolic storage protein breakdown, but presumably are due to biosynthesis in the light. A MapMan representation of transcription of genes related to AA metabolism demonstrates a massive downregulation of genes in the *snrk1α1/α2* mutant, both in AA biosynthesis and catabolism related to most of the AAs (Supplemental Figure S5). Taken together, these results suggest that SnRK1 has a profound impact on AA metabolism during seedling establishment.

SnRK1 controls key catabolic genes facilitating resource mobilization

As we were aiming to elucidate the impact of SnRK1 on transcriptional control during storage compound mobilization, we analyzed the RNA-seq data comparing WT and *snrk1α1/α2* seedlings. Figure 5 summarizes the corresponding SnRK1-dependent genes. Whereas genes in TAG-mobilization (e.g. *SDP1*), glyoxylate cycle (e.g. *CITRATE SYNTHASE1/2*), gluconeogenesis and the tricarboxylic acid cycle (TCA), showed generally no or only marginal SnRK1-dependent changes in transcript levels, distinct genes such as *ACX4* and *PMDH2* involved in β-oxidation displayed strong differences, both in darkness and light. *PCK1*, which encodes an important metabolic hub for channeling FA-derived dicarboxylic acids into gluconeogenesis, was transcriptionally downregulated during late mutant development in darkness (5 dD).

In line with the metabolic analyses, SnRK1 was found to be involved in transcriptional control of AA catabolism. Genes such as *BRANCHED CHAIN AMINO ACID TRANSAMINASE2* (*BCAT2*) or *METHYLCROTONYL-COA CARBOXYLASE SUBUNIT A/B* (*MCCA/B*) were strongly downregulated in *snrk1α1/α2*. The encoded enzymes are involved in Branched Chain Amino Acid (BCAA) catabolism providing Ac-CoA for the TCA cycle and electrons for mitochondrial ATP generation (Ishizaki et al., 2006; Xing and Last, 2017; Pedrotti et al., 2018). Most strikingly, transcription of cy*PPDK*, encoding an essential metabolic hub for feeding AA-derived pyruvate into gluconeogenesis, relies on SnRK1, both in darkness and light. Indeed, a crucial additive function of *PCK1* and *cyPPDK* in Arabidopsis seedling establishment has recently been demonstrated by a mutant approach (Eastmond et al., 2015) and could be confirmed in our hands (Supplemental Figure S6). Hence, these genes provide ideal models for studying SnRK1-dependent transcriptional control.

The TF bZIP63 controls cy*PPDK* transcription downstream of SnRK1

Aiming at characterizing SnRK1 downstream TFs regulating the cy*PPDK* promoter during seedling establishment, we assayed the RNA-seq data sets for similar transcriptional profiles. As BCAA catabolic genes, such as *MCCA*, have been demonstrated to be controlled by bZIP63 during dark-induced starvation (Pedrotti et al., 2018), we hypothesized a similar regulation for *cyPPDK* in seedling establishment. Interestingly, transcriptome and reverse transcription quantitative PCR (RT-qPCR) studies confirmed that *bZIP63*, *MCCA*, cy*PPDK*, and *PMDH2* (Figure 6A) display a highly related transcriptional response. They were strongly induced upon the shift to light, whereas Glc feeding or absence of SnRK1 completely impaired inducibility. This coordinated expression supports a similar regulation of these genes.

To further support that bZIP63 is involved in controlling transcription of metabolic hubs, a *bZIP63* knockout mutant displayed significantly reduced cy*PPDK* and *MCCA* transcript abundance, both 3 DAG in continued darkness and 6 DAG in day/night regime (Figure 6B).

It has been demonstrated that bZIP63 is directly phosphorylated by the SnRK1 kinase in vivo, thereby stimulating heterodimerization with group S_1 bZIP TFs (Mair et al., 2015). Because of the well-known redundancy between the nine members of the C/S_1 bZIP network (Dröge-Laser and Weiste, 2018), we also analyzed higher-order bZIP mutants. The quadruple *bzip1/53/9/63* mutant harbors T-DNA insertions in two C and S_1 bZIP genes each (Dietrich et al., 2011). Accordingly, this mutant displayed strongly reduced cy*PPDK* induction (Figure 6B). This finding suggests that several bZIP factors of the C/S_1 bZIP heterodimerization network impact cy*PPDK* transcription. In contrast, *PCK1* differs considerably in its expression pattern (Supplemental Figure S7A) and *PMDH2* and *PCK1* transcript abundance does not dependent on C/S_1 bZIPs as demonstrated by mutant analyses (Figure 6B; Supplemental Figure S7B). We therefore propose an independent gene regulatory mechanism for these important hubs in TAG mobilization.

To further support bZIP63 as a transcriptional regulator of *cyPPDK*, we performed gain-of-function experiments using a bZIP63 overexpressing line (bZIP63-OE) driven by the 35S promoter and an Est-inducible bZIP63 line (bZIP63-XVE). Analyzing 6-day-old seedlings, transcript abundance of *bZIP63* and *cyPPDK* target genes showed a clear correlation (Supplemental Figure S7C).

The cy*PPDK* promoter is directly targeted by bZIP63

To study the functional interaction of SnRK1 and bZIP63, we applied transient expression in leaf mesophyll protoplasts (Figure 7A). While bZIP63 expression alone showed only a minor activation of the cy*PPDK* promoter-driven GUS reporter, SnRK1α1 co-expression significantly increased reporter activation in a synergistic fashion, indicating co-operation of bZIP63 and SnRK1.

Based on previous results, SnRK1 activity drives bZIP heterodimerization and consequently target gene activation. We therefore assayed nuclear SnRK1 activity using a recently developed in vivo reporter system (Deroover et al., 2016; Sanagi et al., 2021). Seedlings expressing an evolutionary conserved SnRK1/SnF1/AMPK target peptide (rat ACC,

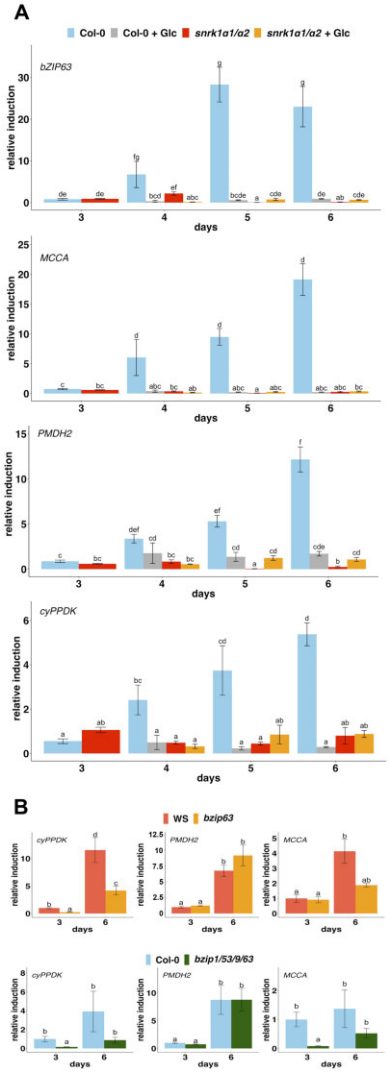

Figure 6 The TF bZIP63 regulates cy*PPDK* transcription. A and B, Transcript abundance of the genes indicated measured by qRT-PCR. A, WT (Col-0, blue) and *snrk1α1/α2* seedlings (red) without or with addition of Glc (gray or orange) were compared 3 DAG in darkness or after shift to 12 h/12 h day/night regime for the time points indicated. B, Relative transcript abundance in WT (WS, red) and *bzip63* (orange) knockout mutants and WT (Col-0, blue) and a quadruple *bzip1/53/9/63* mutant (green) determined after 3 dD and 6 days (3 dD, 3 days 12-h/12-h day/night regime). Given are mean values ±SEM of three biological replicates derived from 15 seedlings relative to WT 3DAG. Significant differences between treatments are designated by letters (one-way ANOVA with Bonferoni–Holm post hoc test; $P < 0.05$).

ACETYL-COA CARBOXYLASE) fused to an N-terminal nuclear localization signal and C-terminal GFP and double HA-tags were analysed for phosphorylation of the ACC peptide using commercial P-ACC antibodies. Quantification reveals an increase in nuclear SnRK1 activity between 3 and 4 DAG, both in darkness and light. Hence, SnRK1 protein levels (Figure 1B) and kinase activity (Figure 7B) are consistent with target gene activation.

TFs controlling cy*PPDK* transcription have not been defined to date. The protoplast system is very well suited to map functional promoter domains. Based on the binding of bZIP63 to G/C-Box (CACGTG/C)-related *cis*-elements (Kang et al., 2010; Kirchler et al., 2010) eight potential binding sites with an ACGT core were identified in the *cyPPDK* promoter. After mutagenesis, these promoters were assayed in protoplasts (Figure 7C).

While mutations in boxes 1 and 5 did not affect the responsiveness to bZIP63 and SnRK1 co-expression, activation was strongly reduced upon mutation in boxes 2, 3, and 6. However, particularly mutations in the boxes 4, 7, and 8 fully impaired effector response. In addition, we performed chromatin Immunoprecipitation coupled to PCR (ChIP-PCR) to study in vivo TF promoter binding in *bzip63* seedlings complemented with a genomic yellow fluorescent protein (YFP)-tagged bZIP63 under control of its own promoter (Figure 7D; Mair et al., 2015). In line with the *cis*-element mapping approach in protoplasts, strong direct binding to the box 4 region of the cy*PPDK* promoter was observed.

In summary, these data provide a mechanistic view of how SnRK1 performs in controlling storage compound mobilization in part through transcriptional reprogramming. As a prototypical example, we demonstrate that SnRK1, via phosphorylation of bZIP63, controls expression of *cyPPDK*, a central metabolic hub for fuelling gluconeogenesis due to AA catabolism (Eastmond et al., 2015).

Discussion

Seedling establishment is a critical stage in the plant's life cycle characterized by highly regulated phase transitions. Sugars, such as Glc, are crucial, both as an energy resource and as signals of metabolic status (Li and Sheen, 2016). In plants, TOR, SnRK1, and HEXOKINASE1 (HXK1) have been identified as major Glc/energy sensing/response systems. For example, upon transition to photoautotrophy, cotyledon-derived Glc has been demonstrated to control root meristematic growth via TOR signaling in a HXK1-independent manner (Xiong et al., 2013).

SnRK1 acts as a central regulator in Arabidopsis storage compound mobilization

Here, we unravel a previously undescribed function of SnRK1 in Arabidopsis seedling establishment, particularly orchestrating TAG and AA resource mobilization during heterotrophic establishment and the transition to an autotrophic phase (Figure 8). The use of an inducible double knockdown approach, addressing redundancy and lethality issues, demonstrated that SnRK1 is required for overall seedling growth and establishment of the photosynthetic apparatus. In line with the previous transcriptome studies in protoplasts (Baena-González et al., 2007) and adult plants (Pedrotti et al., 2018), we observed a massive SnRK1-dependent transcriptional regulation during seedling establishment. Distinct sets of SnRK1-dependent DEGs were found in constant darkness and upon the shift to light. Although these data highlight the plethora of functions

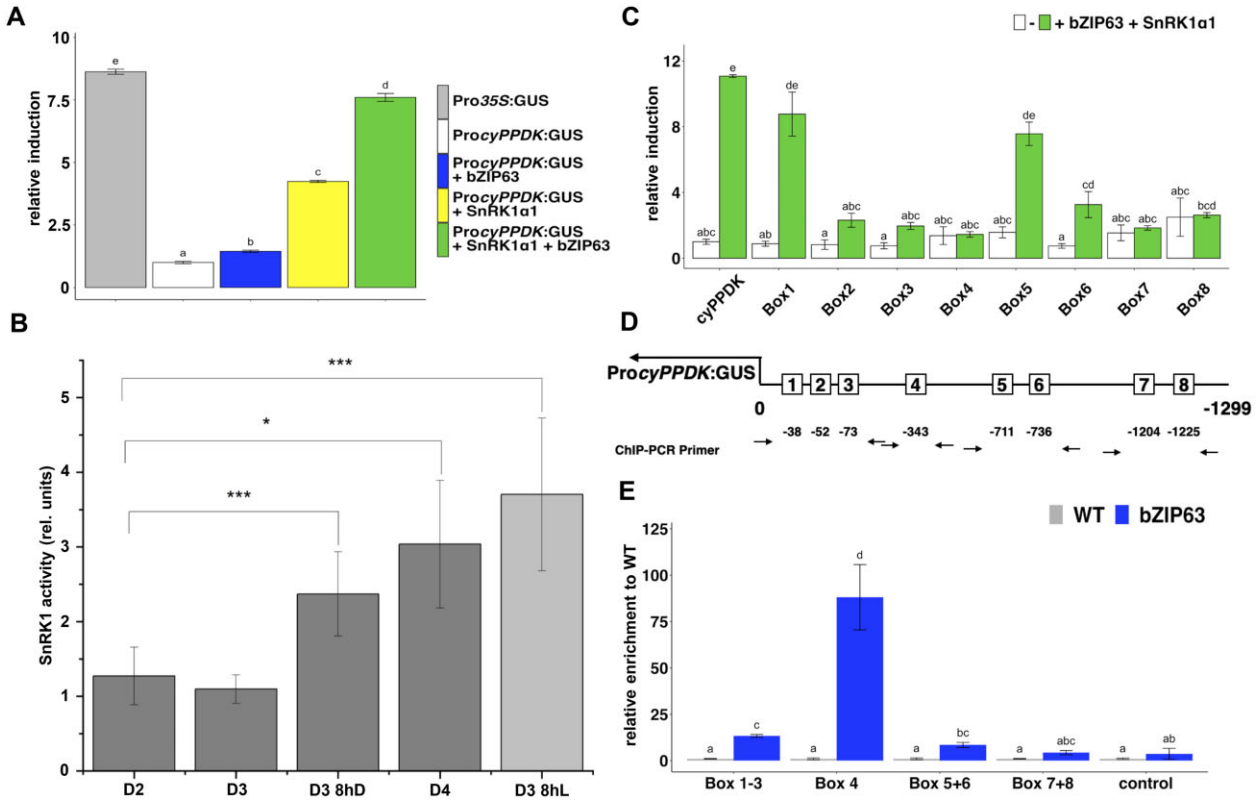

Figure 7 SnRK1 and bZIP63 synergistically control *cyPPDK*, which is a direct target of bZIP63. A, Interplay of SnRK1 and bZIP63 in gene regulation. Leaf mesophyll protoplast transfection assays expressing a Pro*cyPPDK*:GUS reporter (white) and the effectors bZIP63 (blue), SnRK1α1 (yellow) or both (green). Pro*35S*:GUS acts as a positive control. Given are mean values ±SEM of three biological replicates. The experiment was repeated with similar results. B, Nuclear SnRK1kinase activity was determined from seedlings, harvested in the subjective morning in darkness (D2, D3, D4) or 8 h after shift to light (3 D 8hL). Seedlings express a kinase reporter consisting of nuclear localized ACC target peptide fused to GFP and a double HA-tag (Sanagi et al., 2021). ACC-specific phosphorylation was determined relative to the HA-signal using immunoblotting. Given are mean values and SD of three independent experiments. Student's *t* test $^{*}P < 0.05$, $^{**}P < 0.01$, $^{***}P < 0.001$. C, In vivo mapping of potential G-box related binding sites harboring an ACGT core. Non-mutagenized Pro*cyPPDK*:GUS reporter and constructs harboring mutations in the Boxes 1–8 (D) were studied in protoplasts without (white) or after co-expression of bZIP63 and SnRK1α1. Given are mean values (±SEM) of three biological replicates. Induction values are calculated relative to the nonmutagenized reporter as previously described (Ehlert et al., 2006). D and E, $ChIP_{PCR}$ assay to study in vivo binding of *bZIP63:YFP* expressed in 3-day-old *bzip63* seedlings (blue) in comparison to WT (WS, white) using a YFP specific antibody. Due do the close vicinity of some Boxes, the assay cannot discriminate between all neighboring cis-elements. Primer pairs are depicted in the scheme in (D). Given is relative enrichment as mean values ±SEM of three seedling pools (E). Significant differences between treatments are designated by letters (one-way ANOVA with Bonferoni–Holm post hoc test; $P < 0.05$).

performed by SnRK1, feeding with Glc and other metabolizable sugars largely restored defects in mutant growth, chloroplast development, and gene expression. Sugars such as 3-OMG, which are no respiratory substrate and do not contribute to biosynthesis of Glc (Cortés et al., 2003), do not support mutant growth and development. These findings strongly suggest a distinct SnRK1 function in storage resource mobilization. In consequence, a substantial part of the differential gene expression and the observed phenotypical alterations are probably due to limitations in Glc and/or other metabolic resource. It needs to be emphasized that SnRK1 also controls processes beyond the use of storage resources, as revealed by RNAseq experiments after Glc treatment. Moreover, SnRK1-dependent developmental aspects such as hypocotyl elongation or auxin responses require further analyses.

SnRK1 controls TAG degradation on post-transcriptional level and via transcription of hub genes

As an oil-storing plant, Arabidopsis seedling development was proposed to be preferentially fuelled by TAGs (Li-Beisson et al., 2013). Unexpectedly, the TAG content remained constant within the first 3 DAG, but rapidly declined during late seedling development indicating the use of other storage compounds as primary resources. In contrast to published results on TAG mobilization (Gommers and Monte, 2017), our data showed only limited dependency on light but a clear one on SnRK1 function. Protein levels of the catalytic α-subunits as well as kinase activity peaked around 3 DAG, which is preceding the SnRK1-dependent TAG decrease. Whether enzymes involved in TAG degradation are regulated by SnRK1-mediated phosphorylation is currently unknown.

Focused studies on enzymes, selected based on our metabolite and transcriptome profiling, as well as unbiased phosphoproteomic approaches may shed light on this topic. Taken together, late TAG breakdown is clearly SnRK1-dependent and post-translational SnRK1-control of enzymatic activity is very likely.

As our study is focusing on transcriptional regulation, we studied genes in TAG catabolism, particularly controlled by SnRK1. Interestingly, most of the β-oxidation, glyoxylate cycle, or gluconeogenesis genes are hardly/not regulated by SnRK1. Striking exceptions are *PMDH2*, encoding an enzyme for regeneration of NAD^+ to support β-oxidation and *PCK1*, encoding a single, crucial enzyme that facilitates entry of TAG-derived dicarboxylic acids into gluconeogenesis. Hence, instead of coordinated regulation of whole metabolic pathways, our data support a conceptual alternative, namely the regulation of genes encoding crucial bottleneck enzymes.

Sucrose catabolism fuels early seedling establishment in a SnRK1-independent manner

As an unexpected result, substantial amounts of Suc (300 ng/seed) instead of TAGs act as a primary resource fuelling seedling growth during the first DAG. As Fru levels remained low throughout seedling development, it can be assumed that after cleavage of Suc, Fru is rapidly converted into Glc. A coordinated decline of Suc and increase of Glc was observed within 3 DAG, leading to a constant Glc level in WT. Regarding the molar Glc content, a substantial part of the hexoses is used for respiratory purposes.

Suc/Glc ratios have been proposed to function as an important cue to control phase transitions in plants, such as in embryogenesis (Radchuk et al., 2010; Yu et al., 2013). Here, the decline in Suc availability , the abundance of the SnRK1 α-subunits, increase in SnRK1 activity, and the onset of SnRK1 responses correlate in time. It is therefore tempting to propose that sugar signaling controls SnRK1 function in orchestrating seedling establishment. These findings are in line with the nexus model (Figueroa and Lunn, 2016), proposing that trehalose 6-phosphate (T6P) provides information on and controls plant Suc availability. Inhibition of SnRK1 by T6P (Nunes et al., 2013; Figueroa and Lunn, 2016; Zhai et al., 2018) provides a mechanistic mode of action for the metabolic control of SnRK1 activity.

Strikingly, until 5 DAG in light, no impact of SnRK1 on carbohydrate levels was observed, supporting a SnRK1-independent carbohydrate catabolism during early seedling establishment. Along this line, only minor transcriptional regulation of carbohydrate-related metabolic pathways was observed. In the mutant, Glc levels rapidly dropped 6–7 DAG, presumably due to the impaired SnRK1-dependent TAG and AA catabolic activity. In this phase, Glc acts as a central metabolic compound as its depletion results in growth arrest and finally death. In contrast, Glc feeding largely restores growth and chloroplast development.

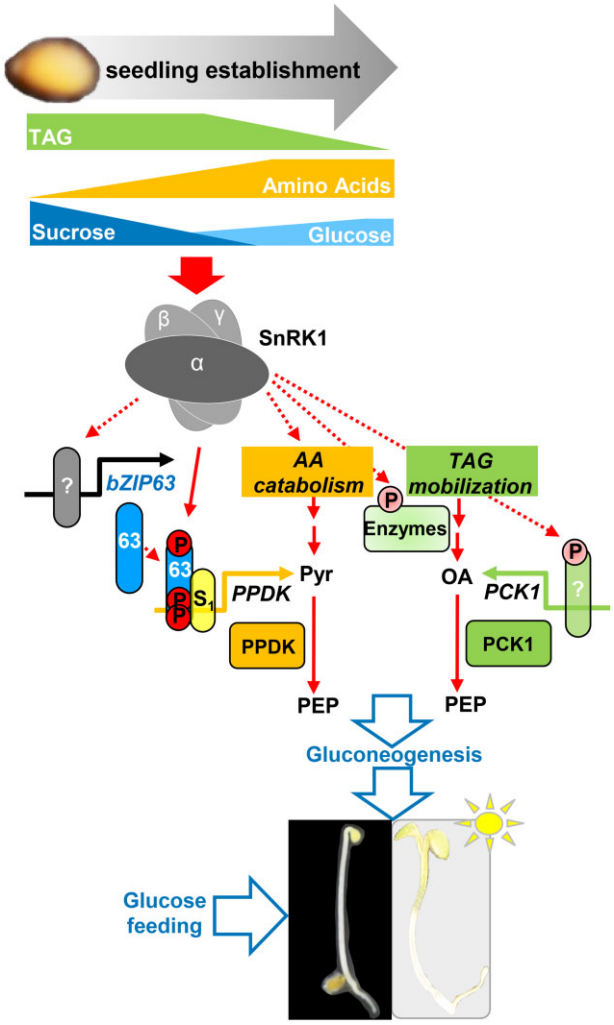

Figure 8 Working model describing the impact of SnRK1 on storage compound mobilization in Arabidopsis seedlings. For details see text. Py, pyruvate; P, phosphate.

SnRK1 orchestrates AA-derived energy metabolism, fuels gluconeogenesis, and facilitates N-mobilization via activation of asparagine biosynthesis

Immediately after germination, the overall AA content increases due to SSP degradation. After reaching a maximum 3 DAG, AA content slightly decreased in darkness, presumably due to catabolic use to fuel energy demands. In contrast, light conditions lead to a significant increase in overall AA content due to biosynthesis. Deficiency in SnRK1 interfered with all these processes, leading to retarded SSP degradation and decreased AA levels. Particularly in light, altered AA levels and gene expression related to AA biosynthesis and catabolism were observed. Strikingly, the high levels of Asn and Gln cannot simply be explained by SSP degradation but are rather caused by de novo biosynthesis. Due to their favorable C/N ratios, they facilitate N-transport to sinks (Lam et al., 2003). Accordingly, important genes such as *ASPARAGINE SYNTHETASE1* (*ASN1*), a well-known SnRK1 target (Baena-González et al., 2007), is transcriptionally downregulated in the mutant. In line with the previous

findings in adult plants (Mair et al., 2015; Pedrotti et al., 2018), transcription of BCAA and Pro catabolic genes (*BCAT2*, *MCCA/B*, *ProDH*) is found to be SnRK1-dependent during seedling establishment. Indeed, the use of BCAAs as a respiratory source is particular advantageous due to its high ATP yield of 29–32 ATP/AA (Hildebrandt et al., 2015). As demonstrated in adult plants, *snrk1α1/α2* mutant studies confirm that the TF bZIP63 is required for BCAA catabolic gene induction during seedling establishment.

SnRK1 controls gluconeogenesis, crucial for seedling establishment, via bZIP63-mediated transcriptional activation of *cyPPDK*

In contrast to animals and yeast, which make use of PYRUVATE CARBOXYLASE (PC) and PHOSPHO*ENOL*PYRUVATE-CARBOXYKINASE (PEPCK, encoded by *PCK* genes) to fuel gluconeogenesis, plants make use of cyPPDK as an essential hub in seedling establishment (Eastmond et al., 2015). Several lines of evidence, based on loss- and gain-of-function experiments, promoter *cis*-element mapping, and ChIP-PCR, confirmed direct binding and synergistic regulation of the cy*PPDK* promoter by SnRK1 and its downstream TF bZIP63. Interestingly, *snrk1α1/α2* mutant analyses confirmed that bZIP63 does not control hub genes in TAG-catabolism (such as *PMDH2* and *PCK1*) and hence specifically coordinates AA catabolism to support gluconeogenesis.

In humans, *PCK* is also controlled at the transcriptional level, integrating multiple hormonal and nutritional cues for hepatic gluconeogenesis (Jitrapakdee, 2012; Zhang et al., 2019). Although the human SnRK1 ortholog AMPK has been implicated in these processes, a mechanistic link to transcription is not well-established. Moreover, a highly complex array of binding sites and cognate TFs has been implicated in human *PCK*-gene regulation. Therefore, additional transcriptional regulators may support bZIP63 in controlling this essential hub gene.

SnRK1 controls bZIP63 via two independent mechanisms (Figure 8). First, the expression of *bZIP63* during seedling establishment is repressed by sugars. Extending previous studies, which excluded participation of the Glc sensor HXK1 in regulation of bZIP63 (Matiolli et al., 2011), our data demonstrate a SnRK1-dependent transcriptional activation via a yet unknown TF. Second, bZIP63 is activated post-translationally by SnRK1 phosphorylation. Mair et al. (2015) identified three SnRK1-dependent in vivo Ser phosphorylation sites in the bZIP63 protein and demonstrated their functional relevance in planta. Indeed, bZIP63 phosphorylation results in induced heterodimerization with group S_1 bZIP factors, which is required for target gene activation. For genes related to BCAA catabolism, stimulus-induced formation of a ternary SnRK1α1-C/S_1-bZIP complex, involved in chromatin remodeling and subsequent gene activation, has been proposed (Weiste and Dröge-Laser, 2014; Mair et al., 2015; Pedrotti et al., 2018). As observed for other C/S_1-bZIP target genes, *bzip63* knockout only partially reduces cy*PPDK* transcription, presumably due to redundancy of the nine C/S_1 bZIP members (Dröge-Laser and Weiste, 2018). Along this line, a quadruple C/S_1-bZIP mutant displays a strong impairment in cy*PPDK* transcript abundance. Several group C and some S_1-members (bZIP1, 2, 11, 44) have been observed to be expressed during seedling establishment (Silva et al., 2016). Hence, identification of bZIP63 heterodimerization partner(s) in the in vivo context is experimentally challenging.

Taken together, SnRK1 performs as a master kinase in seedling establishment orchestrating metabolism and development. With respect to seed storage compound mobilization, it exploits transcriptional regulation of hub genes, such as *cyPPDK* in gluconeogenesis, and presumably post-transcriptional mechanisms, such as control of enzyme activity (Figure 8). In the Arabidopsis model, SnRK1 orchestrates mobilization of TAG and AA reserves. As the composition of storage compounds differs considerably between plant species, pronounced differences in regulation can be anticipated. Comparative studies in appropriate model plants are therefore required to disclose conservation or species-specific differences (Lu et al., 2007). As storage compound mobilization significantly impacts seedling vigor and crop yield (Gommers and Monte, 2017), understanding these regulatory circuits will be instrumental for future crop improvement.

Materials and methods

Plant material

Arabidopsis thaliana ecotypes Columbia (Col-0) or Wassilewskija (Ws) were used as WT controls in this study. The latter was used in studies employing the *bzip63* knockout (ecotype Ws). The *bzip63* (At5g28770) knockout was complemented with a genomic *bZIP63* fragment harboring a C-terminal YFP translational fusion (Mair et al., 2015). The quadruple bZIP T-DNA insertion line (*bZIP1/9/53/63*) combines *bzip1* and *bzip9* knockout with *bzip53* and *bzip63* knockdown mutations (Dietrich et al., 2011). Generation of XVE-bZIP63 was performed according to Weiste and Dröge-Laser (2014). The overexpression line bZIP63-OE is described in Weltmeier et al. (2009). The T-DNA-insertion mutants *snrk1α1-3* (GABI KAT GABI_579E09) and *snrk1α2* were previously published (Baena-González et al., 2007; Mair et al., 2015). An Est-inducible *snrk1α1/α2* double knockdown line was obtained by expression of an amiRNA targeting *SnRK1α2* in a *snrk1α1-3* mutant background (Pedrotti et al., 2018).

Plant growth conditions

Seed germination and seedling establishment were analyzed in a liquid culture system in 24-well plates (Sarstedt, Germany) filled with Murashige and Skoog medium (Skoog et al., 1962) without sugar. WT and mutant seeds were sterilized with chlorine gas and stratified at 4°C for 3–4 days. After a short white light pulse during seedling transfer (10 min) culture was continued in a growth

incubator (Binder, OSRAML30W/865, Lumilux, cool daylight) for 3 dD (21°C, 60% humidity). Afterward plants were shifted to a 12-h light (22°C, 120 µmol $m^{-2}s^{-1}$)/12-h dark (20°C) photoperiod. Samples for determining fresh weight and chlorophyll were harvested immediately after the night phase. Cultivation on soil was performed under similar conditions. Est (10 µM) was added every 3 days as depicted in Figure 1A.

Molecular cloning

Standard DNA cloning techniques were performed as previously described (Sambrook et al., 1989). The Pro*cyPPDK*:GUS (At4g15530) reporter construct used in the transient protoplast transactivation assays was generated by PCR amplifying of a 1,299-bp promoter sequence from Arabidopsis WT genomic DNA using the primers listed in Supplemental Table S1. Making use of the attached restriction sites (*Hind*III, *Nco*I), the promoter fragment was inserted into the reporter plasmid pBT10-GUS (B. Weisshaar, Bielefeld, Germany). For site-directed mutagenesis, G-Box *cis*-elements were mutagenized using the Quick-Change site-directed mutagenesis kit (Stratagene, Amsterdam, Netherlands) following the manufacturer's manual. Primers are listed in Supplemental Table S1.

Plant RNA preparation, RT-qPCR, and RNA-seq

Total plant RNA was prepared from 25 seedlings using an RNeasy Mini Kit (Qiagen, Hilden, Germany) according to the manufacturer's protocol. Quantification of transcript abundance by RT-qPCR was performed using a SYBR green-based detection previously described in Dietrich et al. (2011). Data were obtained from three biological replicates derived from pools of 25 seedlings and normalized to *RRN26* (AtMG00020). All RT-qPCR experiments were repeated at least three times. Oligonucleotide primers are summarized in Supplemental Table S1.

For RNA-seq, 300 ng of total RNA derived from three biological replicates was used for library preparation. Applying Sera-Mag Magnetic Oligo(dT) Particles (Thermo Fisher Scientific, Germany), mRNA was isolated and the cDNA library was prepared using the NEB Next mRNA Library Prep Master Mix Set for Illumina (New England Biolabs, MA, USA) in combination with NEB Next Multiplex Oligos for Illumina (New England Biolabs, MA, USA). RNA quality and fragmentation were checked using an Experion RNA HighSens Analysis Kit (Bio-Rad, CA, USA). During library preparation, products were isolated applying a QIAquick PCR purification kit (Qiagen, Hilden, Germany). For sequencing, six libraries were pooled for each lane of the Illumina Chip. High-throughput sequencing was performed on an Illumina GAIIx platform following the manufacturer's instructions. Quality control of the sequencing data was done using fastQC (http://www. bioinformatics.bbsrc.ac.uk/projects/fastqc/). Mapping of the reads was performed using STAR (Lawrence et al., 2009) onto the Arabidopsis genome release TAIR10. The resulting files were then analyzed applying featureCounts (Liao et al., 2014). For DEG analysis, R was used. Only genes with a *P*-adjust < 0.05 ("BH" correction according to Benjamini and Hochberg) were used for further analysis. For gene ontology (GO) enrichment analysis (Jiao et al., 2012). R (DEseq2 package was used to obtain the list of genes commonly regulated by SnRK1.

SnRK1 kinase assay, SDS–PAGE, and immunoblot

The SnRK1 kinase in vivo reporter assays have been described in (Sanagi et al., 2021). Sodium dodecyl sulphate–polyacrylamide gel electrophoresis (SDS–PAGE) (12%), Coomassie staining for detection of SSPs and immunoblots were previously described (Weiste and Dröge-Laser, 2014). For immune-detection primary polyclonal rabbit-antibodies against SnRK1α1 (1:500 dilution; AS10 919, Agrisera AB, Sweden) or SnRK1α2 (1:1,000 dilution; AS10920, Agrisera AB, Sweden) were used. Moreover, a polyclonal α-ACTIN11 (At3g12110) from mouse (1:1,000 dilution; Agrisera AB, Sweden) and a secondary anti-rabbit antibody (1:10,000 dilution; GE Healthcare) were applied.

Chromatin immunoprecipitation coupled to PCR

For ChIP-PCR, approximately 300 7-day-old seedlings grown on solidified (9 g/L phytoagar) murashige-skoog (MS) medium were harvested after cultivation in darkness for 3 days. WT and a *bzip63* complementation line harboring a genomic *bZIP63* fragment with a translational C-terminal YFP fusion (Mair et al., 2015) were compared. ChIP-PCR was performed as previously described (Weiste and Dröge-Laser, 2014). The data are derived from three biological replicates.

Protoplast isolation and transformation

Protoplast transfection assays were performed according to Yoo et al. (2007) with modifications as described in (Ehlert et al., 2006). β-glucuronidase (GUS) enzyme assays were performed after 16 h of incubation in light (110 $\mu mols^{-1}m^{-2}$). Effector plasmids are given in (Pedrotti et al., 2018).

Determination of chlorophyll content and photochemical efficiency

Twenty-five seeds were frozen in liquid nitrogen, pulverized using a MixerMill (MM400; Retsch) and chlorophyll was extracted with 750 µL of methanol. After incubation at 60°C for 30 min and at room temperature for 10 min, the supernatant was clarified by centrifugation in a bench-top centrifuge and absorption of a 1:10 dilution was measured at 650 and 665 nm in a spectrophotometer. Total chlorophyll content was calculated using the formula: $A_{650} \times 0.025 + A_{665} \times 0.005 \; ¼ =$ mg total chl/mL extract (Porra et al., 1989).

Photochemical efficiency was examined using a plant efficiency analyzer (M-Series MAXI-Version, Walz, Effeltrich, Germany) according to the manufacturer's manual.

Metabolite measurements

For metabolite analysis, three biological replicates were used. Experiments were repeated 2–3 times with similar results. All solvents were at least HPLC grade and were purchased from Biosolve (Valkenswaard, Netherlands). Seeds/seedlings

(n = 25, pooled from one plate) were shock-frozen in liquid nitrogen and extracted for TAG measurements with 2 × 500 µL of chloroform/methanol (2:1, v/v) using a ball mill at 21 Hz for 10 min (Retsch, Haan, Germany). About 0.24 µg of tridecanoyl-TAG (TG30:0 and TG51:0; Larodan, Solna, Sweden) as internal standard (IS) were added. After centrifugation, the organic phase was evaporated in a vacuum concentrator at 40°C. The residue was resuspended in 100 µL isopropanol and analyzed as described (Mueller et al., 2015).

For sugar and AA measurements, plant material was extracted in 50 µl water/acetonitrile (1:1, v/v). Approximately 1.25 µg of D-glucose-6,6-d_2, α,α-trehalose-1,1′-d_2 (both, Sigma Aldrich, Taufkirchen, Germany) and norvaline (2.9 µg) were used as IS. After centrifugation 30 µL were transferred into a high-pressure liquid chromatography (HPLC) vial and analyzed as described in Mueller et al. (2015) with the following MRM transitions: m/z 503→179 at a retention time of 5.33 min for raffinose, m/z 341→179 (5.79 min) for galactinol, (5.26 min) for maltose, (3.91 min) for sucrose, m/z 665→383 (6.65 min) for stachyose, m/z 179→89 (3.27 min) for glucose, (4.99 min) for Fru, m/z 179→87 (4.62 min) for inositol, m/z 181→89 (3.25 min) for D2-glucose (IS) and m/z 343→180 (4.51 min) for D2-trehalose (IS).

For AA measurements, the pellet was reextracted with 50-µL methanol/water (1:1, v/v). After centrifugation, 20 µL of the supernatant from this extraction and 20 µL of the residual plant extract from the sugar measurement were combined, derivatized, and analysed as described (Hartmann et al., 2015).

Quantification and statistical analysis

Statistical tests were all performed using R (https://www.r-project.org/). Significant differences between multiple constructs and treatments were determined using the one-way analysis (ANOVA) of variance test followed by a Bonferroni–Holm post hoc test ($P < 0.05$) and are visualized by different letters. Details are provided in Supplemental Data Set S3.

Accession numbers

RNA-seq data from this article can be found in the Gene Expression Omnibus (GSE183118). Arabidopsis Genome Initiative identifiers for the genes mentioned in this article are as follows: *SnRK1α1/KIN10* (At3g01090), *SnRK1α2/KIN11* (At3g29160), *bZIP63* (At5g28770), *bZIP10* (At4g02640), *bZIP25* (At3g54620), *bZIP9* (At5g24800), *bZIP53* (At3g62420), *bZIP1* (At5g49450), *cyPPDK* (At4g15530), *PCK1* (At3Gg4530), *PMDH2* (At5g09660), *ACX4* (At3g51840), *SDP1* (At5g04040), *ASN1* (At3g47340), *BCAT2* (At1g10070), *MCCA* (At1g03090), *MCCB* (At4G34030), *ProDH1* (At3g30775), *UBI5* (At3g62250), *ACTIN7* (At5g09810), and *ACTIN8* (At1g49240).

Supplemental data

The following materials are available in the online version of this article.

Supplemental Figure S1. Impact of SnRK1 on seedling establishment in darkness.

Supplemental Figure S2. Feeding of metabolic intermediates or amino acids does not rescue the *snrk1α1/α2* mutant phenotype.

Supplemental Figure S3. Impact of SnRK1 on glycerolipid metabolism.

Supplemental Figure S4. Amino acid content in WT and *snrk1α1/α2* seedlings.

Supplemental Figure S5. MapMan representation of genes related to amino acid biosynthesis or catabolism.

Supplemental Figure S6. Phenotype of WT, *ppdk*, *pck1* and *ppdk/pck1* mutants during seedling establishment.

Supplemental Figure S7. Analysis of transcriptional control of *PCK1* and *cyPPDK* during seedling establishment.

Supplemental Table S1. Primers used in this study.

Supplemental Data Set S1. Searchable list of DEGs identified by RNA-Seq.

Supplemental Data Set S2. Metabolites identified by mass spectrometry.

Supplemental Data Set S3. Statistics.

Acknowledgments

We thank Markus Teige (University of Vienna, Austria) and Elena Baena-Gonzalez (IGC Lisbon, Portugal) for providing Arabidopsis seeds. Botany I (University of Würzburg) is acknowledged for access to microscopy and Theresa Damm and Maria Lesch for excellent technical assistance. We thank Franziska Fichtner (University of Queensland, Australia) and Philipp Kreisz (University of Würzburg, Germany) for proof reading.

Funding

This work was supported by the Deutsche Forschungsgemeinschaft (DFG, DR273/18-1).

Conflict of interest statement. None declared.

References

Alonso R, Onate-Sanchez L, Weltmeier F, Ehlert A, Diaz I, Dietrich K, Vicente-Carbajosa J, Dröge-Laser W (2009) A pivotal role of the basic leucine zipper transcription factor bZIP53 in the regulation of Arabidopsis seed maturation gene expression based on heterodimerization and protein complex formation. Plant Cell **21**: 1747–1761

Baena-González E, Rolland F, Thevelein JM, Sheen J (2007) A central integrator of transcription networks in plant stress and energy signalling. Nature **448**: 938–942

Baena-González E, Sheen J (2008) Convergent energy and stress signaling. Trends Plant Sci **13**: 474–482

Baker A, Graham IA, Holdsworth M, Smith SM, Theodoulou FL (2006) Chewing the fat: β-oxidation in signalling and development. Trends Plant Sci **11**: 124–132

Blanco NE, Liebsch D, Guinea Díaz M, Strand Å, Whelan J (2019) Dual and dynamic intracellular localization of Arabidopsis thaliana SnRK1.1. J Exp Bot **70**: 2325–2338

Broeckx T, Hulsmans S, Rolland F (2016) The plant energy sensor: evolutionary conservation and divergence of SnRK1 structure, regulation, and function. J Exp Bot **67**: 6215–6252

Cortés S, Gromova M, Evrard A, Roby C, Heyraud A, Rolin DB, Raymond P, Brouquisse RM (2003) In plants, 3-O-methylglucose is phosphorylated by hexokinase but not perceived as a sugar. Plant Physiol **131**: 824–837

Crepin N, Rolland F (2019) SnRK1 activation, signaling, and networking for energy homeostasis. Curr Opin Plant Biol **51**: 29–36

Deroover S, Ghillebert R, Broeckx T, Winderickx J, Rolland F (2016) Trehalose-6-phosphate synthesis controls yeast gluconeogenesis downstream and independent of SNF1. FEMS Yeast Res **16**: 1–15

Dietrich K, Weltmeier F, Ehlert A, Weiste C, Stahl M, Harter K, Dröge-Laser W (2011) Heterodimers of the Arabidopsis transcription factors bZIP1 and bZIP53 reprogram amino acid metabolism during low energy stress. Plant Cell **23**: 381–95

Dröge-Laser W, Weiste C (2018) The C/S 1 bZIP network: a regulatory hub orchestrating plant energy homeostasis. Trends Plant Sci **23**: 422–433

Eastmond PJ (2006) SUGAR-DEPENDENT1 encodes a patatin domain triacylglycerol lipase that initiates storage oil breakdown in germinating Arabidopsis seeds. Plant Cell **18**: 665–675

Eastmond PJ, Astley HM, Parsley K, Aubry S, Williams BP, Menard GN, Craddock CP, Nunes-Nesi A, Fernie AR, Hibberd JM (2015) Arabidopsis uses two gluconeogenic gateways for organic acids to fuel seedling establishment. Nat Commun **6**: e6659

Ehlert A, Weltmeier F, Wang X, Mayer CS, Smeekens S, Vicente-Carbajosa J, Dröge-Laser W (2006) Two-hybrid protein-protein interaction analysis in Arabidopsis protoplasts: establishment of a heterodimerization map of group C and group S bZIP transcription factors. Plant J **46**: 890–900

Emanuelle S, Doblin MS, Stapleton DI, Bacic A, Gooley PR (2016) Molecular insights into the enigmatic metabolic regulator, SnRK1. Trends Plant Sci **21**: 341–353

Emanuelle S, Hossain MI, Moller IE, Pedersen HL, van de Meene AML, Doblin MS, Koay A, Oakhill JS, Scott JW, Willats WGT, et al. (2015) SnRK1 from Arabidopsis thaliana is an atypical AMPK. Plant J **82**: 183–192

Footitt S, Slocombe SP, Larner V, Kurup S, Wu Y, Larson T, Graham I, Baker A, Holdsworth M (2002) Control of germination and lipid mobilization by COMATOSE, the Arabidopsis omologue of human ALDP. EMBO J **21**: 2912–2922

Figueroa CM, Lunn JE (2016) A tale of two sugars: trehalose 6-phosphate and sucrose. Plant Physiol **172**: 7–27

Gommers CMM, Monte E (2017) Seedling establishment: a dimmer switch-regulated process between dark and light signaling. Plant Physiol **176**: 1061–1074

Graham IA (2008) Seed storage oil mobilization. Annu Rev Plant Biol **59**: 115–412

Hardie DG (2015) AMPK: positive and negative regulation, and its role in whole-body energy homeostasis. Curr Opin Cell Biol **33**: 1–7

Hartmann L, Pedrotti L, Weiste C, Fekete A, Schierstaedt J, Göttler J, Kempa S, Krichke M, Dietrich K, Mueller MJ, et al. (2015) Crosstalk between Two bZIP signaling pathways orchestrates salt-induced metabolic reprogramming in arabidopsis roots. Plant Cell **27**: 2244–2260

Hildebrandt TM, Nunes Nesi A, Araújo WL, Braun H-P (2015) Amino acid catabolism in plants. Mol Plant **8**: 1563–1579

Ishizaki K, Schauer N, Larson TR, Graham IA, Fernie AR, Leaver CJ (2006) The mitochondrial electron transfer flavoprotein complex is essential for survival of Arabidopsis in extended darkness. Plant J **47**: 751–760

Jiao X, Sherman BT, Huang DW, Stephens R, Baseler MW, Lane HC, Lempicki RA (2012) DAVID-WS: A stateful web service to facilitate gene/protein list analysis. Bioinformatics **28**: 1805–1806

Jitrapakdee S (2012) Transcription factors and coactivators controlling nutrient and hormonal regulation of hepatic gluconeogenesis. Int J Biochem Cell Biol **44**: 33–45

Kang SG, Price J, Lin P-CC, Hong JC, Jang J-CC (2010) The Arabidopsis bZIP1 transcription factor is involved in sugar signaling, protein networking, and DNA binding. Mol Plant **3**: 361–373

Kirchler T, Briesemeister S, Singer M, Schütze K, Keinath M, Kohlbacher O, Vicente-Carbajosa J, Teige M, Harter K, Chaban C (2010) The role of phosphorylatable serine residues in the DNA-binding domain of Arabidopsis bZIP transcription factors. Eur J Cell Biol **89**: 175–183

Lam HM, Wong P, Chan HK, Yam KM, Chen L, Chow CM, Coruzzi GM (2003) Overexpression of the ASN1 gene enhances nitrogen status in seeds of Arabidopsis. Plant Physiol **132**: 926–935

Lawrence M, Gentleman R, Carey V (2009) rtracklayer: An R package for interfacing with genome browsers. Bioinformatics **25**: 1841–1842

Li L, Sheen J (2016) Dynamic and diverse sugar signaling. Curr Opin Plant Biol **33**: 116–125

Li-Beisson Y, Shorrosh B, Beisson F, Andresson MX, Arondel V, Bates PD, Baud S, Bird D, Debono A, Durrett TP, et al. (2013) Acyl-lipid metabolism. Arabidopsis Book **11**: e0161

Liao Y, Smyth GK, Shi W (2014) featureCounts: an efficient general purpose program for assigning sequence reads to genomic features. Bioinformatics **30**: 923–930

Lin SC, Hardie DG (2017) AMPK: sensing glucose as well as cellular energy status. Cell Metab **27**: 299–313

Lu C-A, Lin C-C, Lee K-W, Chen J-L, Huang L-F, Ho S-L, Liu H-J, Hsing Y-I, Yu S-M (2007) The SnRK1A protein kinase plays a key role in sugar signaling during germination and seedling growth of rice. Plant Cell **19**: 2484–2499

Mair A, Pedrotti L, Wurzinger B, Anrather D, Simeunovic A, Weiste C, Valerio C, Dietrich K, Kirchler T, Ngele T, et al. (2015). SnRK1-triggered switch of bZIP63 dimerization mediates the low-energy response in plants. eLife **4**: e05828

Matiolli CC, Tomaz JP, Duarte GT, Prado FM, Del Bem LEV, Silveira AB, Gauer L, Corrêa LGG, Drumond RD, Viana AJC, et al. (2011). The Arabidopsis bZIP gene AtbZIP63 is a sensitive integrator of transient abscisic acid and glucose signals. Plant Physiol **157**: 692–705

Mueller SP, Krause DM, Mueller MJ, Fekete A (2015) Accumulation of extra-chloroplastic triacylglycerols in Arabidopsis seedlings during heat acclimation. J Exp Bot **66**: 4517–4526

Nukarinen E, Nägele T, Pedrotti L, Wurzinger B, Mair A, Landgraf R, Börnke F, Hanson J, Teige M, Baena-Gonzalez E, et al. (2016) Quantitative phosphoproteomics reveals the role of the AMPK plant ortholog SnRK1 as a metabolic master regulator under energy deprivation. Sci Rep **6**: 31697

Nunes C, Primavesi LF, Patel MK, Martinez-Barajas E, Powers SJ, Sagar R, Fevereiro PS, Davis BG, Paul MJ (2013) Inhibition of SnRK1 by metabolites: tissue-dependent effects and cooperative inhibition by glucose 1-phosphate in combination with trehalose 6-phosphate. Plant Physiol Biochem **63**: 89–98

Pan R, Liu J, Wang S, Hu J (2020) Peroxisomes: versatile organelles with diverse roles in plants. New Phytol **225**: 1410–1427

Parsley K, Hibberd JM (2006) The Arabidopsis PPDK gene is transcribed from two promoters to produce differentially expressed transcripts responsible for cytosolic and plastidic proteins. Plant Mol Biol **62**: 339–349

Pedrotti L, Weiste C, Nägele T, Wolf E, Lorenzin F, Dietrich K, Mair A, Weckwerth W, Teige M, Baena-González E, et al. (2018). Snf1-RELATED KINASE1-controlled C/S 1 -bZIP signaling activates alternative mitochondrial metabolic pathways to ensure plant survival in extended darkness. Plant Cell **30**: 495–509

Penfield S, Rylott EL, Gilday AD, Graham S, Tony R, Penfield S, Rylott L, Gilday AD, Graham S, Larson TR, et al. (2004). Reserve mobilization in the Arabidopsis endosperm fuels hypocotyl elongation in the dark, is independent of abscisic acid, and requires PHOSPHOENOLPYRUVATE CARBOXYKINASE1. Plant Cell **16**: 2705–2718

Porra RJ, Thompson WA, Kriedemann PE (1989) Determination of accurate extinction coefficients and simultaneous equations for assaying chlorophylls a and b extracted with four different solvents: verification of the concentration of chlorophyll standards by atomic absorption spectroscopy. Biochim Biophys Acta-Bioenerg **975**: 384–394

Pracharoenwattana I, Cornah JE, Smith SM (2007) Arabidopsis peroxisomal malate dehydrogenase functions in β-oxidation but not in the glyoxylate cycle. Plant J. **50**: 381–390

Pracharoenwattana I, Zhou W, Smith SM (2010) Fatty acid beta-oxidation in germinating Arabidopsis seeds is supported by peroxisomal hydroxypyruvate reductase when malate dehydrogenase is absent. Plant Mol Biol **72**: 101–109

Quettier A-L, Eastmond PJ (2009) Storage oil hydrolysis during early seedling growth. Plant Physiol Biochem **47**: 485–490

Radchuk R, Emery RJN, Weier D, Vigeolas H, Geigenberger P, Lunn JE, Feil R, Weschke W, Weber H (2010) Sucrose non-fermenting kinase 1 (SnRK1) coordinates metabolic and hormonal signals during pea cotyledon growth and differentiation. Plant J **61**: 324–338

Ramon M, Dang TVT, Broeckx T, Hulsmans S, Crepin N, Sheen J, Rolland F (2019) Default activation and nuclear translocation of the plant cellular energy sensor SnRK1 regulate metabolic stress responses and development. Plant Cell **31**: 1614–1632

Rylott EL, Gilday AD, Graham IA (2003) The gluconeogenic enzyme phospho*enol*pyruvate carboxykinase in Arabidopsis is essential for seedling establishment. Plant Physiol **131**: 1834–1842

Sambrook J, Fritsch EF, Maniatis TJ (1989) Molecular Cloning: A Laboratory Manual. Cold Spring Harbor Laboratory Press, New York

Sanagi M, Aoyama S, Kubo A, Lu Y, Sato Y, Ito S, Abe M, Mitsutomo A, Mitsuda N, Ohme-Takagi M, et al. (2021). Low nitrogen conditions accelerate flowering by modulating the phosphorylation state of FLOWERING BHLH 4 in Arabidopsis. Proc Natl Acad Sci U S A **118**: e2022942118

Schwacke R, Ponce-Soto GY, Krause K, Bolger AM, Arsova B, Hallab A, Gruden K, Stitt M, Bolger ME, Usadel B (2019) MapMan4: a refined protein classification and annotation framework applicable to multi-omics data analysis. Mol Plant **12**: 879–892

Silva AT, Ligterink W, Hilhorst HWM (2017) Metabolite profiling and associated gene expression reveal two metabolic shifts during the seed-to-seedling transition in Arabidopsis thaliana. Plant Mol Biol **95**: 481–496

Silva AT, Ribone PA, Chan RL, Ligterink W, Hilhorst HWM (2016) A predictive coexpression network identifies novel genes controlling the seed-to-seedling phase transition in Arabidopsis thaliana. Plant Physiol **170**: 2218–2231

Simon NML, Kusakina J, Fernández-López Á, Chembath A, Belbin FE, Dodd AN (2018) The energy-signaling hub SnRK1 is important for sucrose-induced hypocotyl elongation. Plant Physiol **176**: 1299–1310

Skoog M, Murashige T, Skoog F (1962) A revised medium for rapid growth and bioassays with tobacco tissue cultures. Physiol Plant **15**: 473–497

Skylar A, Sung F, Hong F, Chory J, Wu X (2011) Metabolic sugar signal promotes Arabidopsis meristematic proliferation via G2. Dev Biol **351**: 82–89

Tan-Wilson AL, Wilson KA (2012) Mobilization of seed protein reserves. Physiol Plant **145**: 140–153

Tjellström H, Strawsine M, Ohlrogge JB (2015) Tracking synthesis and turnover of triacylglycerol in leaves. J Exp Bot **66**: 1453–1461

Waters MT, Wang P, Korkaric M, Capper RG, Saunders NJ, Langdale JA (2009) GLK transcription factors coordinate expression of the photosynthetic apparatus in Arabidopsis. Plant Cell **21**: 1109–1128

Weiste C, Dröge-Laser W (2014) The Arabidopsis transcription factor bZIP11 activates auxin-mediated transcription by recruiting the histone acetylation machinery. Nat Commun **5**: 3883

Weltmeier F, Rahmani F, Ehlert A, Dietrich K, Schütze K, Wang X, Chaban C, Hanson J, Teige M, Vicente-Carbajosa J, et al. (2009). Expression patterns within the Arabidopsis C/S1 bZIP transcription factor network: availability of heterodimerization partners controls gene expression during stress response and development. Plant Mol Biol **69**: 107–119

Xing A, Last RL (2017) A regulatory hierarchy of the Arabidopsis branched-chain amino acid metabolic network. Plant Cell **29**: 1480–1499

Xiong Y, McCormack M, Li L, Hall Q, Xiang C, Sheen J (2013) Glucose-TOR signalling reprograms the transcriptome and activates meristems. Nature **496**: 181–186

Yoo S-D, Cho Y-H, Sheen J (2007) Arabidopsis mesophyll protoplasts: a versatile cell system for transient gene expression analysis. Nat Protoc **2**: 1565–1572

Yu S, Cao L, Zhou C-M, Zhang T-Q, Lian H, Sun Y, Wu J, Huang J, Wang G, Wang J-W (2013) Sugar is an endogenous cue for juvenile-to-adult phase transition in plants. eLife **2**: e00269

Zhai Z, Keereetaweep J, Liu H, Feil R, Lunn JE, Shanklin J (2018) Trehalose 6-phosphate positively regulates fatty acid synthesis by stabilizing WRINKLED1. Plant Cell **30**: 2616–2627

Zhang X, Yang S, Chen J, Su Z (2019) Unraveling the regulation of hepatic gluconeogenesis. Front Endocrinol (Lausanne). **9**: 1–17